microbial biotechnology

Securing a furan-based biorefinery: disclosing the genetic basis of the degradation of hydroxymethylfurfural and its derivatives in the model fungus *Aspergillus nidulans*

Celso Martins,[1] (iD) Diego O. Hartmann,[1] (iD)
Adélia Varela,[2] (iD) Jaime A. S. Coelho,[3] (iD)
Pedro Lamosa,[1] (iD) Carlos A. M. Afonso[3]** (iD) and
Cristina Silva Pereira[1]* (iD)

[1]*Instituto de Tecnologia Química e Biológica António Xavier, Universidade Nova de Lisboa, Av. da República, Oeiras, 2780-157, Portugal.*

[2]*Instituto Nacional Investigação Agrária e Veterinária, Av. da República, Oeiras, 2784-505, Portugal.*

[3]*Research Institute for Medicines (iMed.ULisboa), Faculty of Pharmacy, Universidade de Lisboa, Av. Prof. Gama Pinto, Lisboa, 1649-003, Portugal.*

Summary

Hydroxymethylfurfural (HMF) is a promising lignocellulosic-derived source for the generation of diverse chemical building blocks constituting an alternative to fossil fuels. However, it remains unanswered if ubiquitous fungi can ensure their efficient decay, similar to that observed in highly specialised fungi. To disclose the genetic basis of HMF degradation in aspergilli, we performed a comprehensive analysis of *Aspergillus nidulans* ability to tolerate and to degrade HMF and its derivatives (including an HMF-dimer). We identified the degradation pathway using a suite of metabolomics methods and showed that HMF was modified throughout sequential reactions, ultimately yielding derivatives subsequently channelled to the TCA cycle. Based on the previously revealed *hmfFGH* gene cluster of *Cupriavidus basilensis,* we combined gene expression of homologous genes in *Aspergillus nidulans* and functional analyses in single-deletion mutants. Results were complemented with orthology analyses across the genomes of twenty-five fungal species. Our results support high functional redundancy for the initial steps of the HMF degradation pathway in the majority of the analysed fungal genomes and the assignment of a single-copy furan-2,5-dicarboxylic acid decarboxylase gene in *A. nidulans*. Collectively our data made apparent the superior capacity of aspergilli to mineralise HMF, furthering the environmental sustainability of a furan-based chemistry.

Introduction

The search for alternative sources of energy and structural building blocks to fossil resources has been recognised as a priority worldwide, and one of the major technological quests during the last decade (Rosatella *et al.*, 2011; van Putten *et al.*, 2013). To alleviate the harmful environmental footprint of the overexploitation of fossil reservoirs, the development of cleaner alternatives is required, safeguarding the health of Earth ecosystems and, consequently, of future generations (Frade *et al.*, 2014).

Lignocellulose, especially its composing polymers lignin, cellulose and hemicellulose, are the frontrunners in the biorefinery of the future. Cellulose and hemicellulose can be used as carbon source in fermentation processes for the production of ethanol (Delidovich *et al.*, 2014). Their hydrolytic degradation at high temperatures releases the composing sugar monomers; yet cellulose is less amenable to hydrolysis than hemicellulose (which does not form crystalline regions). The resulting monomers, namely hexoses and pentoses, can be subsequently converted through dehydration to 5-hydroxymethylfurfural (HMF) and furfural (FF) respectively (Rosatella *et al.*, 2011). Importantly, HMF can also be obtained directly from fructose or from glucose *via*

isomerisation to fructose (van Putten *et al.*, 2013; Zhang and Dumont, 2017). Both renewable resources, HMF and FF, have already been used to successfully generate a considerable array of chemical building blocks (van Putten *et al.*, 2013). Due to the ease of production of HMF and its derivatives, it has been estimated that they will rapidly reach a global scale of use (Rosatella *et al.*, 2011; van Putten *et al.*, 2013; Resasco *et al.*, 2015; Zhang and Dumont, 2017). The potential absence of cytotoxic effects of several building blocks derived from HMF has been suggested before using a human cell line at defined concentration and exposure time (Frade *et al.*, 2014).

In the context of biorefinery, some studies have reported HMF inhibitory effects on the growth of bacteria (Franden *et al.*, 2013; Wang *et al.*, 2014) or yeasts (Taherzadeh *et al.*, 2000; Wang *et al.*, 2013) during industrial fermentation processes. This led to the characterisation of HMF reduction to 2,5-bis(hydroxymethyl)furan (BHMF) or oxidation to 5-(hydroxymethyl)furan-2-carboxylate (HMFCA) by several yeasts during the production of ethanol (Yuan *et al.*, 2020). The inhibitory effects of both FF and HMF during the conversion of lignocelluloses to ethanol, and how they influence the expression of central metabolism-related genes (e.g. pentose phosphate pathway or TCA cycle) have been extensively analysed (Liu *et al.*, 2004; Gorsich *et al.*, 2006; Hristozova *et al.*, 2006; Liu, 2006; Hristozova *et al.*, 2008; Yuan *et al.*, 2020). Recently, the biotechnological potential of two bacteria – *Acinetobacter oleivorans* and *Serratia marcescens* – to transform HMF into added-value compounds, namely BHMF, furan-2,5-dicarboxylic acid (FDCA) or HMFCA, was described (Godan *et al.*, 2019; Muñoz *et al.*, 2020). In addition, the diversity of metabolites formed during the transformation of HMF (as well as FF) by *Amorphotheca resinae* ZN1 (Ran *et al.*, 2014) – also known as the 'creosote fungus' (Seifert *et al.*, 2007) – was characterised. The biodegradation pathway in this fungus was proposed to be similar to that of the bacterium *Cupriavidus basilensis* for which the composition of the HMF degradation gene cluster (*hmfFGH* gene cluster) was originally fully assigned (Koopman *et al.*, 2010). This know-how opened doors to generate bioengineered strains for the production of valuable HMF-derivatives, and to screen for other organisms suitable for HMF-biotransformation. Filamentous fungi, particularly *Aspergillus flavus*, have been proposed for the production of FDCA through the transformation of HMF (Rajesh *et al.*, 2019), and a US-patent targeting the genetic transformation of fungi for the production of FDCA was also recently conceded (De Bont *et al.*, 2018). The transcription of genes coding for enzymes putatively involved in the degradation/detoxification pathway of HMF was already comprehensively analysed in

Pleurotus ostreatus (Feldman *et al.*, 2015) and *A. resinae* (Wang *et al.*, 2015; Yi *et al.*, 2019), though the genetic assignment of FDCA transformation that links HMF degradation to the central metabolism, remains unknown.

Our aim was to verify the capacity of aspergilli, specifically of *A. nidulans* – a ubiquitous Ascomycota that plays a key role in the degradation of lignocelluloses (Martins *et al.*, 2019) – to degrade and/or modify HMF. Accordingly, we systematically analysed the degradation pathway of HMF and of several building blocks derived from it (Fig. 1) using chromatography, spectrometry and spectroscopy methods. To characterise the genetic basis of this pathway in *A. nidulans,* we relied on expression of genes homologous to the *hmfFGH* cluster of *C. basilensis* and on their functional analyses in single-deletion mutants, as well as, on orthology analyses to scrutinise their prevalence, conservation and specificity across fungi.

Results and discussion

Toxicity of HMF and its derivatives against A. nidulans: determination of inhibitory values

The concentrations of FF, HMF and of the building blocks derived from HMF (Fig. 1) capable to inhibit 50% of *A. nidulans* growth (IC_{50}) were determined (depicted in Table 1). FF was the second least toxic compound against the fungus, contradicting the observed high toxicity against *Candida* spp., *Pichia stipitis* and *Saccharomyces cerevisiae* (Taherzadeh *et al.*, 2000; Liu *et al.*, 2004; Gorsich *et al.*, 2006; Hristozova *et al.*, 2006; Liu, 2006; Hristozova *et al.*, 2008; Wang *et al.*, 2013). All the tested HMF-based chemicals (placed on the right of FF in Table 1) showed lower toxicity against *A. nidulans* compared to HMF, except for 5-(chloromethyl)furan-2-carbaldehyde (CMF, $IC_{50} < 1$ mM). These results reinforce that the chemical modification of HMF can potentially reduce the ecotoxicity of the ensuing derivatives, as often reported for other chemicals (Voutchkova-Kostal *et al.*, 2012). The exception being CMF that is a man-made chemical (obtained either from HMF, glucose or cellulose) and not a biotransformation product of HMF as the remaining tested compounds (Capuano and Fogliano, 2011). The high toxicity of CMF (Table 1) and potential mutagenicity reported before (Surh and Tannenbaum, 1994) challenge the idea that CMF can replace HMF as a major chemical structural building block (Mascal, 2015).

We selected HMF, furan-2,5-diyldimethanol (BHMF), furan-2,5-dicarboxylic acid (FDCA) and 5,5'-diformylfurfuryl ether (OBMF) to characterise, under co-metabolic conditions, the degradation pathway of HMF in *A. nidulans*. In the biodegradation assays (5 ml cultures) at
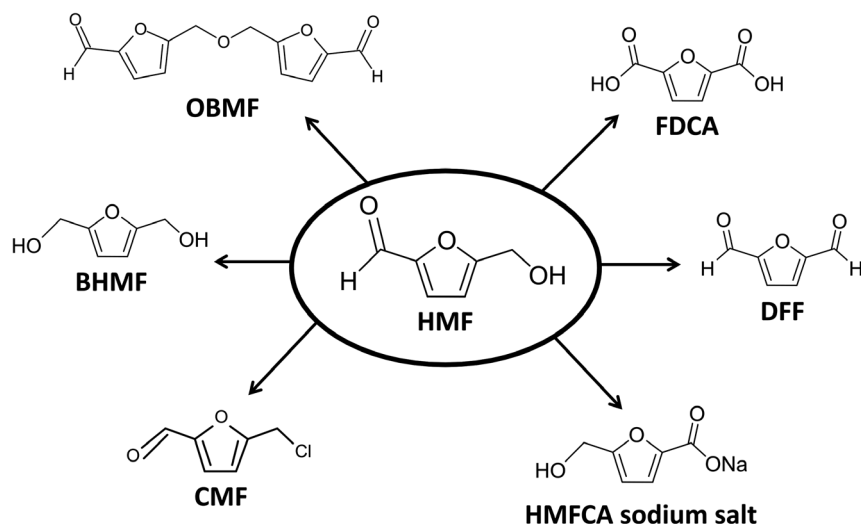
Fig. 1. Relevant building blocks obtained from HMF.

Table 1. IC$_{50}$ values obtained for each compound displayed both in mass (mg ml^{-1}) and molarity (mM). The underlined chemicals were the ones selected for biodegradation experiments.

	LA	FA	Furfural	DFF	Na-HMFA	CMF	HMF	BHMF	FDCA	OBMF
IC$_{50}$ (mg ml^{-1})	0.22	4.43	1.68	0.62	0.33	0.14	0.19	0.54	0.39	0.44
IC$_{50}$ (mM)	1.93	45.19	17.12	4.99	1.99	0.97	1.51	4.18	2.49	1.89

concentrations matching the estimated IC$_{50}$ values (Table 1), a reduction to half in the mycelial biomass (fresh weights) compared to the control at the fourteenth day of incubation was consistently observed (Fig. S1).

Biodegradation of HMF and its derivatives

The capacity of *A. nidulans* to degrade HMF or its derivatives was analysed by monitoring the residual concentration of each parental compound in media, daily until the seventh day of incubation and at the fourteenth day (Fig. 2). The concentrations (mM) of HMF, BHMF, FDCA and OBMF quantified along the incubation time are depicted in Fig. 2A–D respectively. None of the compounds suffered abiotic degradation (i.e. in negative controls without the fungus; Figs S2–S5). HMF and OBMF were readily degraded by *A. nidulans* as both compounds disappeared from the growth media after one and two days of incubation respectively (Fig. 2A and D). BHMF degradation by the fungus was stepwise; its concentration in the medium decreased very rapidly during the first day of incubation, afterwards disappearing at a slower rate until the seventh day of incubation when virtually all the compound was eliminated from the media (Fig. 2B). The least biodegradable compound was FDCA (Fig. 2C, continuous line) since the maximum degradation level was below 20%, reaching a steady value after the first day of incubation.

Glucose has been previously reported to repress the production of fungal enzymes expected to participate in the degradation of FDCA, such as decarboxylases or cellulases (Xiao *et al.*, 2004; Li *et al.*, 2012). Consistent results were attained when testing *in vitro* the decarboxylation of FDCA by a decarboxylase or a cellulase, both significantly impaired when glucose was added to the reaction medium (Fig. S6, full details in Supplementary Information). To bypass the glycolysis pathway, we tested FDCA biodegradability in medium supplemented with acetate, which is channelled directly to the TCA cycle, instead of glucose. In the acetate-based medium, the degradation of FDCA by the fungus surpassed 40%, being almost steady from the first day onwards (Fig. 2C, dotted line). Overall, the biodegradability assays (Fig. 2) support the ability of *A. nidulans* to detoxify media supplemented with HMF or its derivatives, even if their degradation may be under carbon catabolite repression.

We also analysed the diversity of the metabolites formed during the biodegradation of HMF, BHMF, FDCA or OBMF (co-metabolic conditions with glucose; Fig. 2). Quantification was only done for the degradation intermediates which accumulated extracellularly; whenever present intracellularly their detection could be validated but levels were below the quantification limits. The metabolites were identified by liquid chromatography, that is comparison of the retention time and the UV spectrum with that of a chemical standard. To validate
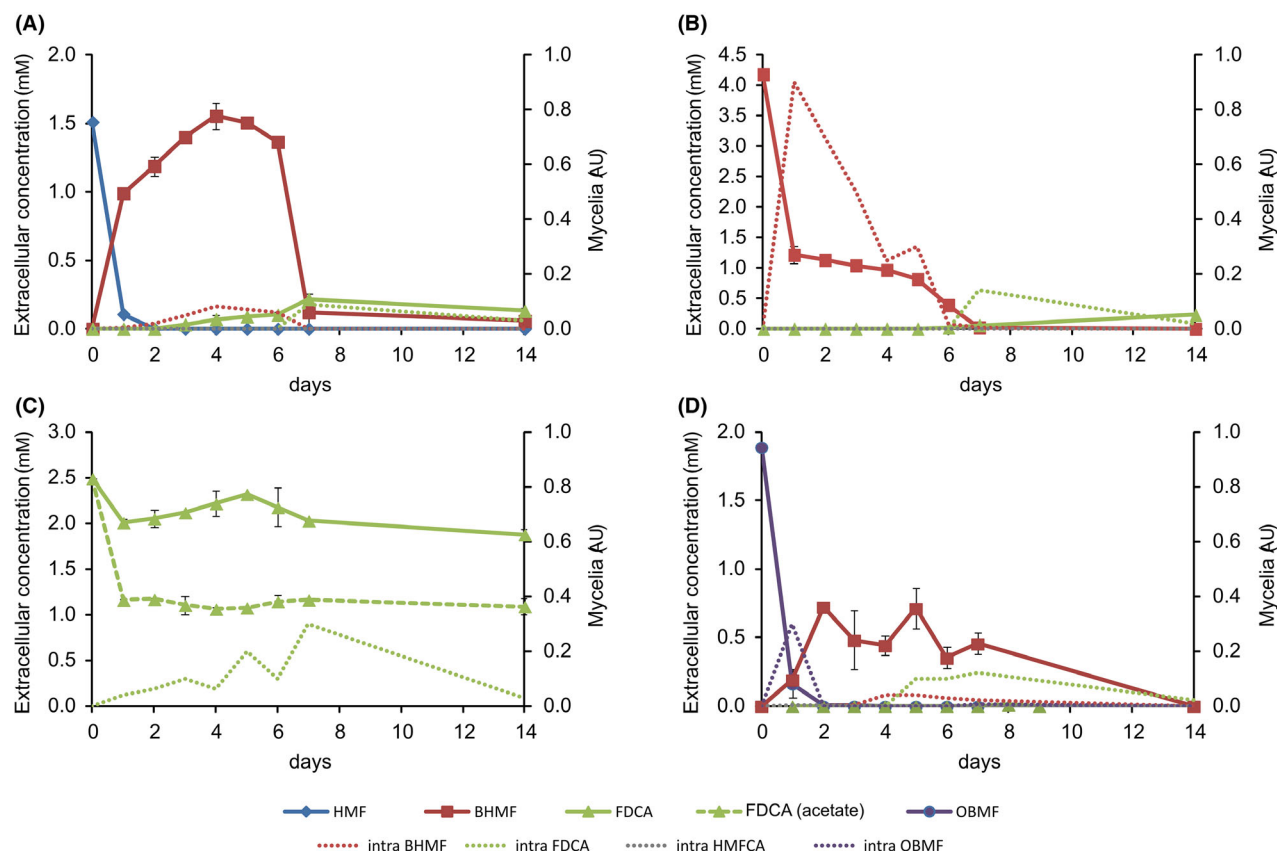
Fig. 2. Biodegradability of HMF and its derivatives along the incubation time in *A. nidulans* submerged cultures. The growth media (MMG) were supplemented with the IC_{50} concentration of HMF (A), BHMF (B), FDCA (C) or OBMF (D) and their extracellular concentrations measured daily during the first 7 days and after 14 days (mM). The chromatographic detection of specific transformation products along the incubation time is also depicted comprising both extracellular (continuous lines, mM) and intracellular (dotted lines, arbitrary units) sub-products. FDCA biodegradability was reassessed also in MM supplemented with acetate instead of glucose (C, dashed line).

the identification of the metabolites, we have also resorted to ^{1}H NMR when above its detection threshold. Glucose was totally consumed at the fifth day of incubation (NMR data, Figs S2–S5).

In the conditions of the study, the HMF supplemented to the medium was converted by the fungus to BHMF, FDCA, HMFCA and furoic acid (FCA; Fig. 2A, Table S1 and Fig. S2). All compounds were detected by liquid chromatography except FCA which was detected only by NMR (Table S1). BHMF and FDCA were detected in both fractions, although their quantifications were only possible in the extracellular fraction (Fig. 2A). BHMF accumulated in the growth medium at the first day of incubation prior to its appearance in the mycelium at the fourth day (Fig. 2A). At the seventh day, BHMF concentration in medium greatly decreased and FDCA started to accumulate in both fractions (Fig. 2A). Along the entire course of HMF degradation by the fungus, HMFCA was systematically detected in the medium (Table S1). FDCA conversion is likely intracellular since

its levels were kept stable in the medium until the end of the incubation, yet decreasing in the mycelia. Finally, FDCA was converted into FCA which was found in the medium at the fourteenth day of incubation (Table S1). HMFCA conversion into FDCA has been suggested before during degradation of HMF by *A. resinae* (Ran *et al.*, 2014), regardless that FDCA was not detected in this early study. The proposed degradation pathway of HMF in *A. nidulans* is depicted in Fig. 3A.

The disappearance of the exogenously supplemented BHMF from the culture medium was essentially due to its cellular uptake (detected in the mycelia from the first time point; Fig. 2B, Table S1 and Fig. S3). Similar to that observed during the degradation of HMF by the fungus, at the half-point of incubation, the disappearance of BHMF matched the appearance of FDCA at low amounts in both fractions (detected by HPLC and ^{1}H-NMR).

FDCA biotransformation (exogenously added to the cultures, medium with glucose) was less than 20% at
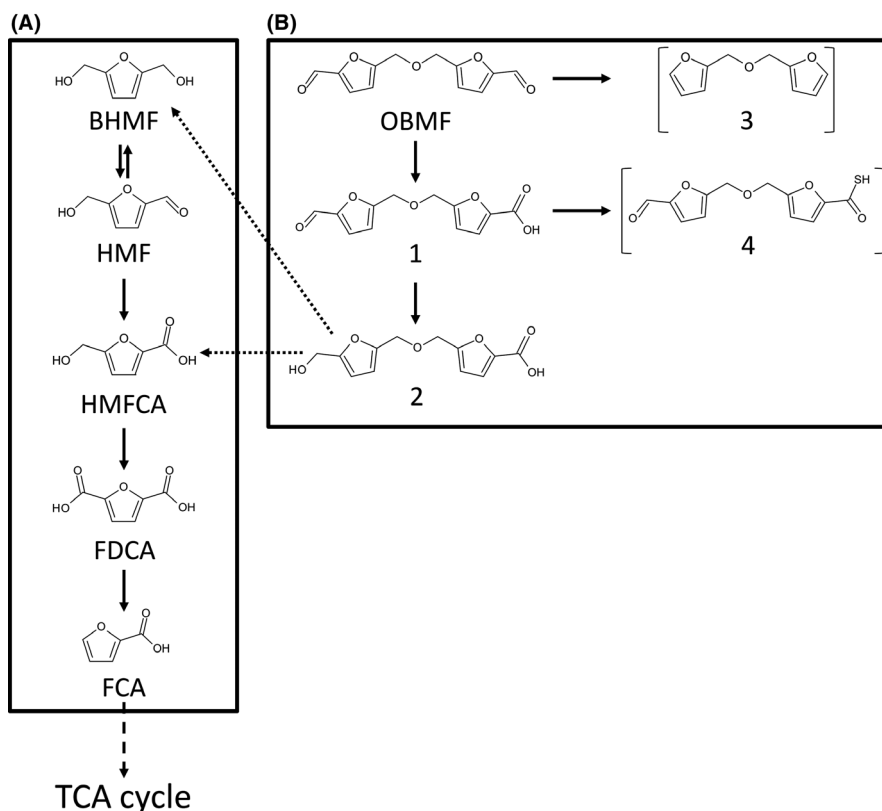
Fig. 3. Schematic representation of the HMF degradation pathway based on the results obtained in this work and adapted from Ran and colleagues (2014) (A). Proposed pathway of transformation of OBMF based on the results obtained in this work (compounds in brackets were not confirmed by MS/MS analysis) (B).

the end of the incubation (Fig. 2C). The fungus internalised FDCA (Table S1 and Fig. S4) and possibly also converted it to FCA even if unseen in these samples. As mentioned above, the transformation of FDCA by *A. nidulans* is apparently the slowest step in the degradation pathway of HMF (Fig. 3A).

Finally, we have undertaken a mechanistic study of the biodegradability of OBMF (a dialdehyde formed by HMF dimerisation) to evaluate the potential environmental persistence of HMF-based polymers. OBMF removal from the culture medium (exogenously added) was completed in only two days of incubation (Fig. 2D), resulting in a rapid extracellular accumulation of HMFCA (below the quantification limit) and BHMF, and late mycelial accumulation of BHMF and FDCA (Fig. 2D and Table S1). However, major unknown peaks were also observed in the chromatograms (Fig. S5). The NMR data showed the accumulation of two major degradation intermediates – non-symmetric molecules – that consistently increased along the incubation (Fig. 2D, and Fig. S5). To refine their chemical structures, the last incubation point (extracellular medium) was also analysed by LC-ESI-MS. We have focused our analysis on the major intensity peak (ca. 3.36 min) of the total ion

chromatogram (TICs; $\pm$ 0.1 min) that display masses with signal intensity above 10^5 (Fig. S7, Supplementary Data 1.xlsx). The retrieved ion masses matched two identifications: 5-{[(5-formylfuran-2-yl)methoxy]methyl}furan-2-carboxylic acid (M = 250 g mol^{-1}; compound 1) and 5-({[5-(hydroxymethyl)furan-2-yl]methoxy}methyl)furan-2-carboxylic acid (M = 252 g mol^{-1}; compound 2; Figs S8–S11). Compound identities were confirmed against the MS/MS spectra of standard compounds (synthesis and characterisation details in the Supplementary Information, Figs S8–S15). Two other intermediates could be suggested based on matching exact masses yet no confirmation was possible due to high error (above 10ppm): 5-{[(5-formylfuran-2-yl)methoxy]methyl}-furan-2-carbothioic *S*-acid (M = 266 g mol^{-1}; compound 3) and 2,2'-[oxybis(methylene)]difuran (M = 178 g mol^{-1}; compound 4; Supplementary Data 1.xlsx). Based on these results, we can propose that one aldehyde group of OBMF is oxidised yielding compound 1, followed by the reduction of the remaining aldehyde yielding compound 2 (Fig. 3B). The ether linkage of compound 2 is cleaved yielding BHMF and HMFCA that are subsequently channelled to the HMF degradation pathway. Regardless of low accuracy at the LC-ESI-MS analyses

(outside confidence interval), one can hypothesise that as secondary reactions, OBMF is converted to compound 3 (decarbonylation reaction), and compound 1 converted to compound 4 (introduction of a thiol (-SH) group).

Transcriptional profile of A. nidulans *genes putatively involved in HMF biodegradation*

The *hmfFGH* gene cluster was previously described in *C. basilensis*, relying on the functional characterisation of single-gene deletion mutants during HMF degradation (Koopman *et al.*, 2010). The authors demonstrated that *hmfH* – a FAD-dependent oxidoreductase – catalyses the transformation of HMF to BHMF (reversible reaction), as well as the sequential conversion of HMF to HMFCA and then to FDCA. In addition, *hmfF* and *hmfG* were shown to code for decarboxylases that mediate the conversion of FDCA to FCA. Based on the BLAST analysis best-hits (NCBI), three putative homologous genes were identified in the genome of *A. nidulans*, namely AN7164 (Score = 72.4, E-Value = $9E^{-14}$), AN12147 (Score = 112, E-Value = $7E^{-31}$) and AN4212 (Score = 205, E-Value = $5E^{-58}$) with sequence similarity to *hmfF*, *hmfG* and *hmFH* respectively (Table S2). InterProScan analyses showed that both AN7164 and AN12147 genes code for proteins with a predicted decarboxylase domain, whereas AN4212 encodes a protein with a FAD/NADP dependent oxidoreductase domain (Table S2, see protein domain details Figs S16–S21). Therefore, targeted gene expression assays (*q*RT-PCR) were conducted to assess if these genes responded upon exposure to HMF, BHMF or FDCA. We also analysed the expression of AN12148, a gene coding for a putative transcription factor that in previous versions of *A. nidulans* genome was annotated together with AN12147 as a single gene (AN7163).

The observed steady increase of the expression of AN4212 along time, upon exposure to HMF, supports that this gene encodes an enzyme involved in the conversion of HMF (Fig. 4, Table S4). However, upon exposure to BHMF, this gene showed an erratic expression response that suggests the involvement of other genes coding in the transformation of BHMF to HMF. These results are consistent with the hypothesis raised by Ran and colleagues (2014), in which the transformation of HMF is mediated by an aldehyde oxidoreductase (possibly the same for both HMF conversion steps: HMFCA and BHMF), while the transformation of BHMF to HMF is likely conducted by a alcohol dehydrogenase (ADH), yet to be disclosed. It can be hypothesised that in *A. nidulans*, BHMF yields HMF due to the activity of an unknown ADH; HMF is subsequently oxidised to HMFCA and then to FDCA at a very slow conversion rate (Figs 2 and 3). The low FDCA conversation rate, together with the much higher toxicity of both HMF and HMFCA compared to BHMF (Table 1), may result in the usage of BHMF as a rescue low toxicity compound in *A. nidulans* similar to that proposed for *A. resinae* (Ran *et al.*, 2014). Importantly, upon exposure to FDCA, the AN4212 gene underwent down-regulation, but the AN7164 gene showed a steady increase along time that is consistent with its predicted decarboxylase function (Fig. 4, Table S4). Moreover, AN7164 expression levels were kept low upon exposure to HMF or BHMF, reinforcing its specificity to FDCA (Fig. 4, Table S4). The observed low increase of AN7164 expression levels upon exposure to BHMF possibly reflects the formation of low amounts of FDCA. The observed AN12147 gene expression levels were not significantly increased in any of the tested conditions, including upon exposure to HMF, suggestive that this gene does not participate in the HMF degradation pathway (Fig. 4, Table S4). The AN12148 gene (a putative transcription factor in an array with AN12147 and AN7164) showed high expression levels in control conditions (glucose) or upon exposure to either HMF or BHMF, but underwent a noteworthy down-regulation upon exposure to FDCA. Based on the acquired expression data (Fig. 4, Table S4), at this stage, we cannot link this gene with HMF degradation pathway. We have attempted to generate the corresponding single-gene deletion mutant that was however not viable, suggesting that AN12148 is an essential gene (data not shown).

To confirm the assignments done for AN4212 and AN7164 genes in *A. nidulans*, we generated the corresponding single-gene deletion mutants, subsequently characterising their ability to degrade HMF or FDCA (Fig. 5A and B). In the presence of glucose, none of the deletion mutants was impaired in their capacity to degrade HMF that was completely removed after seven days of incubation. Both mutants during HMF degradation accumulated extracellularly BHMF and FDCA (below 0.2 mM; Fig. 5A), similar to that observed in the wild-type strain (Fig. 2). When glucose was replaced by acetate, both mutants accumulated extracellularly only BHMF (0.66–0.76 mM; Fig. 5A). Acetate is channelled directly to the TCA cycle, resulting in a $NAD(P)^+/NAD(P)H$ imbalance that favours reduction reactions (Minard and McAlister-Henn, 2009), hence consistent with the observed accumulation of BHMF in this condition. This observation deserves further analysis in the near future, especially as BHMF constitutes a sustainable alternative to adipic acid, alkyldiols or hexamethylenediamine as a building block for the synthesis of polymers (Zhang and Dumont, 2017). The transformation of FDCA is a slow step in *A. nidulans* (Fig. 2), mostly due to its high dependence on the upstream oxidation/reduction steps.
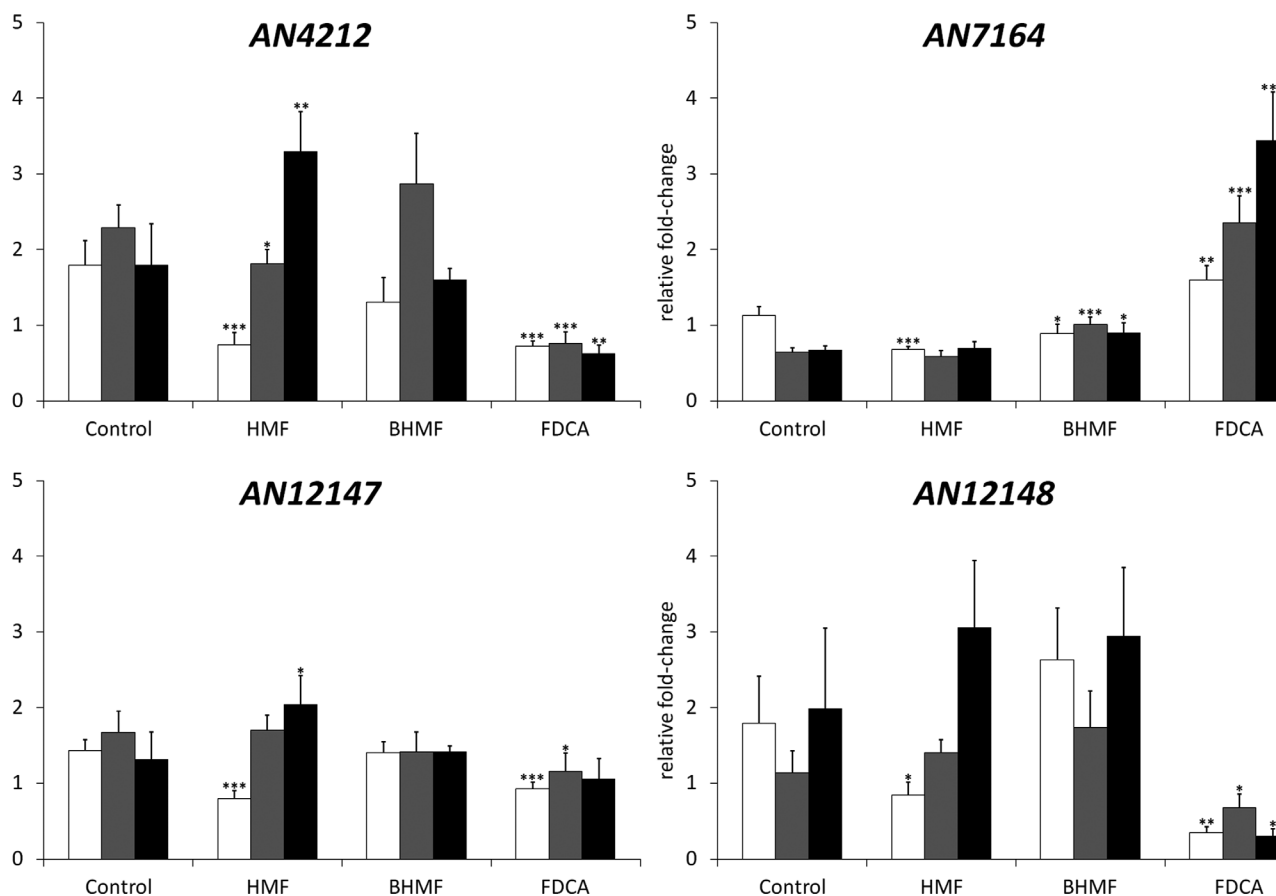
Fig. 4. Relative expression of genes putatively involved in HMF, BHMF and FDCA transformation (AN4212, AN7164, AN12147 and AN12148), determined by *q*RT-PCR. *Aspergillus nidulans* was exposed to HMF, BHMF or FDCA for 30 (white), 60 (grey) or 120 min (black). The y axes represent the fold-change of gene expression relative to time zero (before exposure). β-tubulin gene was used as internal control. The asterisks mark significant difference in expression of treatment when compared to the control for each exposure time (*$P < 0.05$; **$P < 0.01$, ***$P < 0.001$).

Finally, we exposed the AN7164 deletion mutant to FDCA (IC_{50} concentration) growing in acetate medium (Fig. 5B). No transformation of FDCA was detected; contrariwise, we observed a decay of more than 50% of FDCA in the wild-type strain cultures, consistent with our previous observations (Fig. 2). Our data revealed that in *A. nidulans* the decarboxylation of FDCA involves a specific enzyme that is encoded by the gene AN7164 (Fig. 5C).

Orthology analysis of key genetic elements of HMF degradation pathway across fungi

A orthology study across the genomes of 25 fungi representative of major taxonomic classes was conducted to analyse the widespread genetic potential of fungi to transform HMF (Supplementary Data 2.xlsx). Proteins from different organisms carrying the same functional domain and of which the encoding genes are orthologous, likely display the same enzyme-functionality

(Emms and Kelly, 2019). The results show the presence of 212 oxidoreductase genes orthologous to the AN4212 gene (orthogroup; Table S7, Supplementary Data 3). Some fungi contain several paralogous genes in their genomes, of which the more gifted is *P. ostreatus* ($n = 40$), followed by five *Aspergillus* spp., namely *A. flavus* ($n = 19$), *A. nidulans* ($n = 14$), *A. niger* ($n = 15$), *A. sydowii* ($n = 14$) and *A. versicolor* ($n = 15$; Table S7, Supplementary Data 2.xlsx and Supplementary Data 3). Consistent with the functional redundancy of this orthogroup in *A. nidulans* ($n = 14$), the deletion of AN4212 did not affect the mutant capacity to transform HMF (Fig. 5). This orthogroup contains the *A. resinae* genes M430DRAFT_35707, M430DRAFT_57262 and M430DRAFT_59892 (Arz_18116_T1, Arz_11534_T1 and Arz_16765_T1 in the publication, respectively; Wang *et al.*, 2015) and the *P. ostreatus* transcripts 69649, 82653, 93955, 114510, 116309, 121882 (Feldman *et al.*, 2015; Table S7, Supplementary Data 3). Both sets of genes were previously reported to play roles in the
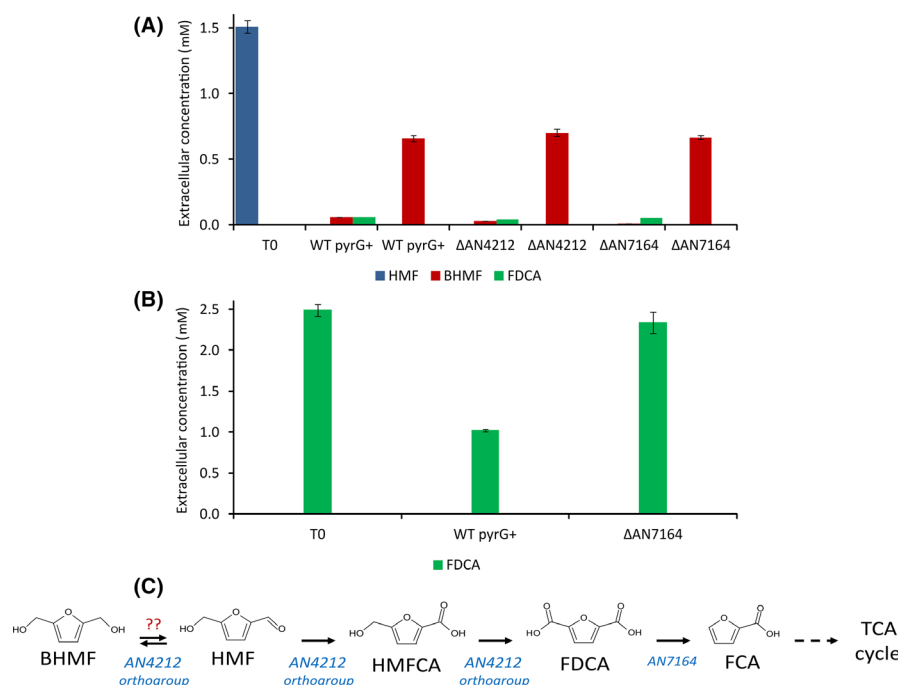
Fig. 5. Products formed after 7 days of incubation with IC_{50} concentration of HMF in glucose or acetate (marked as underlined) media by *Aspergillus nidulans* wild type (WT *pyrG*[+]) and the mutants ΔAN4212 and ΔAN7164 (A); and with IC_{50} concentration of FDCA in acetate medium by WT *pyrG*[+] and the mutant ΔAN7164 (B). Only the molecules of which the identification could be validated using HPLC (RT and spectra) and ^{1}H-NMR, and within the HPLC method quantification limits, are shown. The schematic representation of the HMF degradation pathway for *A. nidulans* is also displayed (C).

transformation of HMF (Feldman *et al.*, 2015; Wang *et al.*, 2015). The observed widespread presence of the AN4212 orthogroup suggests that the genetic basis of the initial transformation steps of HMF is conserved across distinct fungal classes. Consistent results were shown by protein alignments within the AN4212 orthogroup (full details in Supplementary Information and Supplementary Data 5).

The AN7164 orthogroup comprises 26 genes (Table S7, Supplementary Data 4) and is present in only 13 of the 25 analysed genomes, of which seven were *Aspergillus* spp.. AN7164 is a single copy gene in the genome of *A. nidulans*, yet multi copies were found in *Fusarium oxysporum* ($n = 5$), *A. aculeatus* ($n = 3$), *A. niger* ($n = 3$), *A. sydowii* ($n = 3$), *A. flavus* ($n = 2$), *A. terreus* ($n = 2$) and *Trichoderma virens* ($n = 2$; Table S7, Supplementary Data 2.xlsx and Supplementary Data 4). High conservation across the AN7164 orthogroup was also noticed at the level of the protein sequence alignments (full details in Supplementary Information and Supplementary Data 6). Based on this, one can speculate that aspergilli possibly play important roles in the environmental mineralisation of FDCA. We found that *A. resinae* – capable to decarboxylate FDCA to FCA under aerobic conditions (Ran *et al.*, 2014) – contains in the genome only one gene orthologous to AN7164, while no orthologous were found in the genome of *P. ostreatus*.

FDCA decarboxylation to FCA was verified in *A. nidulans* cultures where transient low levels of FCA could be detected (Table S1). Based on our results, we propose AN7164 as a furan-2,5-dicarboxylic acid decarboxylase in *A. nidulans*.

Conclusions

The potential of HMF as a lignocellulosic-derived source for the innovative generation of diverse chemical building blocks is often announced as peerless, recently projected to soon reach a global scale of use (Rosatella *et al.*, 2011; van Putten *et al.*, 2013; Delidovich *et al.*, 2014). Improved mechanistic understandings of the impact of HMF and its derivatives on the environment are necessary to further guide the development of a furan-based biorefinery and the choice of sustainable production modes and products. Our work further emphasises fungi as valuable tools for a furan-biorefinery: *A. nidulans* degrades HMF-based chemicals (including an unusual dialdehyde) under co-metabolic conditions that can be modulated to generate different metabolites. Taken as examples, simply by altering the carbon source in the growth medium, HMF mineralisation can be hindered leading to BHMF accumulation, or FDCA conversion rate to FCA altered. FDCA was identified by US Department of Energy as one of 10 priority

chemicals for establishing the 'green' chemistry industry of the future (Bozell and Petersen, 2010).

Several oxidoreductases belonging to the AN4212 orthogroup were found widespread in the analysed fungal genomes, including in *A. nidulans* ($n = 14$), consistent with the observed capacity of the corresponding single-deletion mutant to still transform HMF. The AN4212 orthogroup contains *A. resinae* genes and *P. ostreatus* genes that were previously linked to HMF transformation, suggestive of genetic conservation of the first steps of this pathway across distinct fungal classes. Our results allowed the assignment of the AN7164 as a furan-2,5-dicarboxylic acid decarboxylase gene in *A. nidulans*. All the seven well-known aspergilli saprobes analysed here – that greatly contribute for the environmental degradation of lignocelluloses (Martins *et al.*, 2019) – contain the genes required for HMF mineralisation using a similar degradation pathway to that previously define in *A. resinae* (Ran *et al.*, 2014). The nonexistence of genes orthologous to AN7164 in nearly half of the analysed fungal genomes (including in *P. ostreatus*) reinforces the specificity of this decarboxylation step, regardless that the existence of different FDCA transformation routes deserves further analysis. Our results support the potential utility of fungi for the development of novel biotreatments seeking production of sustainable chemical building blocks and as environmental sentinels of the safeness of a future 'furan-based biorefinery'.

Experimental procedures

Chemicals

Levulinic acid (LA), furfuryl alcohol (FA) and furan-2-carbaldehyde (furfural, FF) were purchased from Merck (Germany). The remaining chemicals, furan-2,5-dicarbaldehyde (DFF), sodium 5-(hydroxymethyl)furan-2-carboxylate (Na-HMFA), 5-(chloromethyl)furan-2-carbaldehyde (CMF), 5-hydroxymethyl-2-furaldehyde (HMF), 2,5-bis(hydroxymethyl)furan (BHMF), furan-2,5-dicarboxylic acid (FDCA), 5,5'-diformylfurfuryl ether (OBMF), were synthesised as previously described (Coelho *et al.*, 2014; Frade *et al.*, 2014).

Growth medium

A minimal medium was used containing *per* litre 1 g K_2HPO_4 (pH 7.0, autoclave sterilised) plus 3 g $NaNO_3$, 0.01 g $ZnSO_4.7H_2O$, 0.005 g $CuSO_4.5H_2O$, 0.5 g $MgSO_4.7H_2O$, 0.01g $FeSO_4.7H_2O$ and 0.5 g KCl (sterilised by filtration prior to use). Glucose (1%) was added to the minimal medium, hereafter referred as MMG.

Toxicology assays

To establish the inhibitory concentration of 50% of the fungal growth (IC_{50}), 96-well plates were prepared using twofold dilutions of each chemical in MMG, reaching a final volume of 200 μl. The concentrations ranged from 5.40 to 0.02 mg ml^{-1} in the cases of LA, HMF, DFF, CMF, Na-HMFA, BHMF, FDCA and OBMF. For FA, the values ranged from 108.00 to 0.42 mg ml^{-1} and for FF between 36.30 and 0.14 mg ml^{-1}. The growth media were inoculated with *Aspergillus nidulans* FGSC A4 reaching a concentration of 5×10^5 spores ml^{-1}, prepared as described before (Martins *et al.*, 2014) and incubated at 30 °C. Two independent experiments were run, each in triplicates along with abiotic (non-inoculated medium, containing the tested chemicals) and biotic (inoculated medium containing no chemicals) controls. Fungal growth was measured daily (absorbance at 600 nm) using an Infinite M200 spectrophotometer (Tecan, Switzerland). The results were registered whenever the positive control reached the stationary phase (stable absorbance values, in this experiment after 72 h of incubation), as previously described (Petkovic *et al.*, 2009). The inhibition values were then calculated and adjusted using a logistic regression computed using the XL-STAT software version 2009.1.02 (Addinsoft, France).

Biodegradation experiments

A set of compounds, namely HMF, BHMF, FDCA and OBMF, were considered for the biodegradation experiments; the first two due to their emerging central role in biorefinery and the last two largely due to their novelty (Coelho *et al.*, 2014). The fungal cultures (MMG containing the test compounds at the above established IC_{50} values) were grown in 6-well plates (5 ml per well), using as inocula *A. nidulans* spores (5×10^5 spores ml^{-1}) incubated at 30 °C with gentle agitation (100 rpm). Two independent experiments were run, each in triplicates, along with abiotic and biotic controls. Biodegradation was assessed at discrete time points: daily from day 1 to 7, and then at day 14. At each time point, the cultures were harvested, separating the mycelia from the extracellular medium through vacuum filtration. The fresh mycelia were weighted in the last time point (14 days). Both, medium and mycelia, were frozen (−20 °C) until further analysis. To evaluate if glucose could hinder the capacity of the fungus to degrade FDCA, an additional experiment was conducted in MM media supplemented with the IC_{50} of FDCA where acetate (150 mM) was used as carbon source instead of glucose.

Extraction

Mycelial samples were extracted using a fast solvent-based protocol. Briefly, 10 ml of 50% water/methanol (v/v) *per* gram of sample was added to the mycelia (frozen with liquid nitrogen and grounded using mortar and

pestle), mixed and then placed on an ultrasonic bath during 15 min. The samples were then centrifuged (15 min 10 000 *g*) and the supernatant recovered. The pellet was re-extracted using the same ratio *per* sample of 100% methanol, and the remaining steps repeated. The combined supernatants were dried under gentle nitrogen flow and stored at −20 °C until further analysis.

Liquid chromatography

The extracellular fractions (with methanol, 50% sample/methanol, v/v) and intracellular extracts (re-suspended in 200 μl methanol) were analysed with an Acquity Ultra-Performance Liquid Chromatograph (Waters, Milford, MA, USA) with PDA detector. Data were collected and processed with the Empower software. The injections were made using a 10 μl loop operated in partial-loop mode. Compounds separations were achieved on a Waters Symmetry column, 5 μm (4.6 × 250mm) thermostated at 27 °C and the samples maintained at 4 °C. The mobile phase consisted on ultra-pure water (Merck Millipore, Darmstadt, Germany; eluent A) and acetonitrile (eluent B), with a flow rate of 0.8 ml min⁻¹. The analyses of FDCA used an isocratic method with 5% of eluent B, an injection of 10 μl, UV detection at 275 nm. For the remaining compounds (HMF, BHMF, OBMF and Na-HMFA) a gradient method was used with the same eluents as follows: eluent B is increased from 1% to 50% in 20 min, which was held for 5 min before return, in 2 min, to the initial conditions and then re-equilibrated for 8 min (total run time was 35 min); with a flow rate of 0.9 ml min⁻¹. The injection volumes varied between 5 μl (OBMF), 10 μl (HMF) and 20 μl (BHMF and Na-HMFA), and the UV detection of the compounds was performed at 235 and 260 nm. An external quantification method was used and the quantification limits were 0.01 mg ml⁻¹ for HMF and FDCA, and 0.05 mg ml⁻¹ for BHMF and OBMF.

Nuclear magnetic resonance spectroscopy

Freeze-dried material was dissolved in 900 μl of deuterated water and 15 μl of KOH 10 M for NMR analyses. All spectra were acquired on a Bruker AVANCE III 800 spectrometer (Bruker, Rheinstetten, Germany) working at a proton operating frequency of 800.33 MHz, equipped with a four channel 5 mm inverse detection probe head with pulse-field gradients along the Z-axis. Spectra were run at 25 °C using standard Bruker pulse programs. ^{1}H spectra were acquired with water pre-saturation during the relaxation delay.

Mass spectrometry

Aliquots of the extracellular medium of the fungal cultures grown in MMG with OBMF were analysed by microLC-MS using a Triple TOF 6600 MS system (Sciex) equipped with the DuoSprayTM ion source. Chromatographic separation was carried out in the Eksigent ekspert nanoLC425 in microflow using an HALO C18 (50 mm × 0.5 mm, 2.7 μm particle sizes, 90 Å) column from Eksigent at the flow rate of 10 μl min⁻¹. The mobile phase consisted of a solution of 0.1% formic acid (solvent A) and a solution of acetonitrile containing 0.1% formic acid (solvent B), set as follows: 20% B in 2 min, followed by a linear gradient of 20–95% B in 12 min, 2 min of 95% B, 2 min to return to the initial conditions and 5 min to re-equilibrate the column. MS was operated in negative ionisation mode, with TOF MS scan with an *m/z* range 100–1000 for 500 ms for a total cycle time of 0.5 s. MS data were processed using the PeakView software using the extracted-ion chromatogram for the compounds of interest. For compound identity, a $\Delta(m/z) \leq 10$ ppm, as well as a low noise/signal ratio, was considered.

Experimental conditions for gene expression analysis

To obtain robust and clean *q*RT-PCR results it is important to test gene expression in young and fresh mycelia, in opposition to the longer incubation times performed during the biodegradation assays. Therefore, *A. nidulans* was pre-grown during 48 h in 6-well plates (5 ml per well), using the above described MMG as initial medium, inoculated with spores (5×10^5 spores ml⁻¹) and incubated at 30 °C with gentle agitation (100 rpm). Then, the medium was removed and the formed mycelia carefully washed with saline solution prior to the addition of MM containing HMF, BHMF or FDCA as sole carbon sources. The mycelia were recovered by filtration (0.45 μm membrane filters, Millipore) after 30, 60 and 120 min of exposure to each compound, immediately frozen in liquid nitrogen.

Total RNA extraction and cDNA synthesis

Approximately 50 mg of mycelia was grounded with poly (vinylpyrrolidone; 0.4 mg per mg of mycelia) with a mortar and pestle. The final powder was used in the extraction and purification of total RNA using the RNeasy Plant Mini Kit (QIAGEN), according to the manufacturer's protocol. Genomic DNA digestion was done with the RNase-Free DNase Set (QIAGEN). Quality, integrity and quantity of the total RNA were analysed in a NanoDrop 1000 Spectrophotometer (Thermo Fisher Scientific, Waltham, MA, USA) and by running 2 μg of RNA into 1% agarose gels in TBE (Tris-boric acid-EDTA) buffer. The complementary DNA (cDNA) was synthesized from 1000 ng of the total RNA using an iScript cDNA Synthesis Kit (Bio-Rad) in T1000 Thermal

Cycler (Bio-Rad, Hercules, CA, USA). The reaction protocol consisted of 5 min at 25 °C, 30 min at 42 °C and 5 min at 85 °C.

Quantitative real-time PCR analysis

For gene expression analysis, oligonucleotide pairs for specific *A. nidulans* genes (Table S3) were designed using the GenScript web tool (https://www.genscript.com/tools/real-time-pcr-taqman-primer-design-tool) and produced by STAB Vida Lda. (Portugal). The *q*RT-PCR analysis was performed in a CFX96 Thermal Cycler (Bio-Rad), using the SsoFast EvaGreen Supermix (Bio-Rad), 250 nM of each oligonucleotide and the cDNA template equivalent to 10 ng of total RNA, at a final volume of 10 μl per well, in three technical replicates. The PCR conditions were as follows: enzyme activation at 95 °C for 30 s; 40 cycles of denaturation at 95 °C for 10 s and annealing/extension at 59 °C for 15 s; and melting curve obtained from 65 to 95 °C, consisting of 0.5 °C increments for 5 s. Data analyses were performed using the CFX Manager software (Bio-Rad). The expression of each gene was taken as the relative expression compared to the time zero (before incubation with the tested compounds). The expression of all target genes was normalized by the expression of β-tubulin gene (*tubC*, AN6838), used as internal control. Five biological replicates were performed. Statistical analyses of the *q*RT-PCR data were performed in the GraphPad Prism v6.0 software. Expression values from cultures incubated with HMF, BHMF or FDCA were compared with the control for every respective incubation time by multiple Student's *t*-tests. Differences in gene expression with a *P*-value below 0.05 were considered statistically significant.

Generation and analyses of single-gene deletion mutants

Genes AN4212 or AN7164 were selected for replacement with *A. fumigatus pyrG* gene (*pyrG*[Afu]) in an *Aspergillus nidulans* A1149 auxotrophic strain (*pyrG*−). The generation of the single-deletion mutant strains for this study (Table 2) was performed according to a previously established method (Hartmann *et al.*, 2019) that is detailed in Supplementary Information. Briefly, deletion cassettes were constructed by fusion PCR, combining the 5' and 3'-flanking regions of each target gene with *pyrG*[Afu]. *Aspergillus nidulans* A1149 protoplasts were produced, transformed with each cassette and plated onto selective media. Isolated transformants (twelve for AN4212 and eight for AN7164) were cultivated on selective media for three generations to assure stable mutations. DNA from each transformant was extracted, and

Table 2. The *Aspergillus nidulans* strains used in this study.

Strains	Genotype	Source
A4	wild type, *veA*+	FGSC[a]
A1149	*pyrG89*; *pyroA4*; *nkuA*::*argB*	FGSC[a]
A1149 *pyrG*+	*pyrG89*; *pyroA4*; *nkuA*::*argB*; *pyrG89*::*pyrG*[Afu]	Hartmann and colleagues (2019)
ΔAN4212	*pyrG89*; *pyroA4*; *nkuA*::*argB*; ΔAN4212::*pyrG*[Afu]	This study
ΔAN7164	*pyrG89*; *pyroA4*; *nkuA*::*argB*; ΔAN7164::*pyrG*[Afu]	This study

a. Fungal Genetics Stock Center.

diagnostic PCR was performed for each gene. Based on amplicon size, it was possible to confirm correct gene replacement of the transformants. Further confirmation was attained by restriction enzyme digestion (BglII and NdeI) of the PCR products and analyses of the digestion patterns of mutant and wild-type strains (Fig. S22 and S23). One confirmed single-deletion mutant for each gene was selected to be further studied. Mutant and control strains were incubated with IC_{50} concentrations of HMF or FDCA up to 7 days in glucose or acetate media and the degradation products were determined as described above.

Computational analyses

The genomes (translated transcripts – protein FASTA format) of most of the selected fungal species were downloaded from the FungiDB database (release 46; Stajich *et al.*, 2012), with the exception of the genome of *A. resinae* which was downloaded from the Ensembl database (release 100; Yates *et al.*, 2020), and of *P. ostreatus* which was downloaded from the Joint Genome Institute database (release 8.18.47; Grigoriev *et al.*, 2014). Functional domain analysis to the genome of *A. nidulans* was performed using InterProScan v5.44-79.0 (Jones *et al.*, 2014). Full genome orthology studies, including the generation of gene trees, were performed using OrthoFinder v2.3.11 (Emms and Kelly, 2015, 2017, 2018, 2019). The gene trees were visualised and graphically edited with FigTree v1.4.4.

Acknowledgements

Conflict of interest

The authors declare that they have no conflict of interest.

References

Bozell, J.J., and Petersen, G.R. (2010) Technology development for the production of biobased products from biorefinery carbohydrates—the US Department of Energy's "Top 10" revisited. *Green Chem* **12**: 539–554.

Capuano, E., and Fogliano, V. (2011) Acrylamide and 5-hydroxymethylfurfural (HMF): a review on metabolism, toxicity, occurrence in food and mitigation strategies. *LWT–Food Sci Technol* **44**: 793–810.

Coelho, J.A., Trindade, A.F., Andre, V., Duarte, M.T., Veiros, L.F., and Afonso, C.A. (2014) Trienamines derived from 5-substituted furfurals: remote epsilon-functionalization of 2,4-dienals. *Org Biomol Chem* **12**: 9324–9328.

De Bont, J.A.M., Ruijssenaars, H.J., and Werij, J. (2018) *Fungal Production of FDCA*. Gorinchem, the Netherlands: Purac Biochem B.V.

Delidovich, I., Leonhard, K., and Palkovits, R. (2014) Cellulose and hemicellulose valorisation: an integrated challenge of catalysis and reaction engineering. *Energy Environ Sci* **7**: 2803–2830.

Emms, D.M., and Kelly, S. (2015) OrthoFinder: solving fundamental biases in whole genome comparisons dramatically improves orthogroup inference accuracy. *Genome Biol* **16**: 157.

Emms, D.M., and Kelly, S. (2017) STRIDE: species tree root inference from gene duplication events. *Mol Biol Evol* **34**: 3267–3278.

Emms, D., and Kelly, S. (2018) STAG: species tree inference from all genes. *BioRxiv* 267914.

Emms, D.M., and Kelly, S. (2019) OrthoFinder: phylogenetic orthology inference for comparative genomics. *Genome Biol* **20**: 1–14.

Feldman, D., Kowbel, D.J., Glass, N.L., Yarden, O., and Hadar, Y. (2015) Detoxification of 5-hydroxymethylfurfural by the *Pleurotus ostreatus* lignolytic enzymes aryl alcohol oxidase and dehydrogenase. *Biotechnol Biofuels* **8**: 63.

Frade, R.F.M., Coelho, J.A.S., Simeonov, S.P., and Afonso, C.A.M. (2014) An emerging platform from renewable resources: selection guidelines for human exposure of furfural-related compounds. *Toxicol Res* **3**: 311.

Franden, M.A., Pilath, H.M., Mohagheghi, A., Pienkos, P.T., and Zhang, M. (2013) Inhibition of growth of *Zymomonas mobilis* by model compounds found in lignocellulosic hydrolysates. *Biotechnol Biofuels* **6**: 99.

Godan, T.K., Rajesh, R., Loreni, P.C., Rai, A.K., Sahoo, D., Pandey, A., and Binod, P. (2019) Biotransformation of 5-hydroxymethylfurfural by *Acinetobacter oleivorans* S27 for the synthesis of furan derivatives. *Bioresour Technol* **282**: 88–93.

Gorsich, S.W., Dien, B.S., Nichols, N.N., Slininger, P.J., Liu, Z.L., and Skory, C.D. (2006) Tolerance to furfural-induced stress is associated with pentose phosphate pathway genes ZWF1, GND1, RPE1, and TKL1 in *Saccharomyces cerevisiae*. *Appl Microbiol Biotechnol* **71**: 339–349.

Grigoriev, I.V., Nikitin, R., Haridas, S., Kuo, A., Ohm, R., Otillar, R., *et al.* (2014) MycoCosm portal: gearing up for 1000 fungal genomes. *Nucleic Acids Res* **42**: D699–D704.

Hartmann, D.O., Piontkivska, D., Moreira, C.J., and Silva Pereira, C. (2019) Ionic liquids chemical stress triggers sphingoid base accumulation in *Aspergillus nidulans*. *Front Microbiol* **10**: 864.

Hristozova, T., Angelov, A., Tzvetkova, B., Paskaleva, D., Gotcheva, V., Gargova, S., and Pavlova, K. (2006) Effect of furfural on carbon metabolism key enzymes of lactose-assimilating yeasts. *Enzyme Microb Technol* **39**: 1108–1112.

Hristozova, T., Gotcheva, V., Tzvetkova, B., Paskaleva, D., and Angelov, A. (2008) Effect of furfural on nitrogen assimilating enzymes of the lactose utilizing yeasts *Candida blankii* 35 and *Candida pseudotropicalis* 11. *Enzyme Microb Technol* **43**: 284–288.

Jones, P., Binns, D., Chang, H.-Y., Fraser, M., Li, W., McAnulla, C., *et al.* (2014) InterProScan 5: genome-scale protein function classification. *Bioinformatics* **30**: 1236–1240.

Koopman, F., Wierckx, N., de Winde, J.H., and Ruijssenaars, H.J. (2010) Identification and characterization of the furfural and 5-(hydroxymethyl)furfural degradation pathways of *Cupriavidus basilensis* HMF14. *Proc Natl Acad Sci USA* **107**: 4919–4924.

Li, J., Wang, J., Wang, S., Xing, M., Yu, S., and Liu, G. (2012) Achieving efficient protein expression in *Trichoderma reesei* by using strong constitutive promoters. *Microb Cell Fact* **11**: 84.

Liu, Z.L. (2006) Genomic adaptation of ethanologenic yeast to biomass conversion inhibitors. *Appl Microbiol Biotechnol* **73**: 27–36.

Liu, Z.L., Slininger, P.J., Dien, B.S., Berhow, M.A., Kurtzman, C.P., and Gorsich, S.W. (2004) Adaptive response of yeasts to furfural and 5-hydroxymethylfurfural and new chemical evidence for HMF conversion to 2,5-bis-hydroxymethylfuran. *J Ind Microbiol Biotechnol* **31**: 345–352.

Martins, I., Garcia, H., Varela, A., Núñez, O., Planchon, S., Galceran, M.T., *et al.* (2014) Investigating *Aspergillus nidulans* secretome during colonisation of cork cell walls. *J Proteomics* **98**: 175–188.

Martins, T.M., Martins, C., and Silva Pereira, C. (2019) Multiple degrees of separation in the central pathways of the catabolism of aromatic compounds in fungi belonging to the Dikarya sub-Kingdom. *Adv Microb Physiol* **75**: 177–203.

Mascal, M. (2015) 5-(Chloromethyl) furfural is the new HMF: functionally equivalent but more practical in terms of its production from biomass. *ChemSusChem* **8**: 3391–3395.

Minard, K.I., and McAlister-Henn, L. (2009) Redox responses in yeast to acetate as the carbon source. *Arch Biochem Biophys* **483:** 136–143.

Muñoz, T., Rache, L.Y., Rojas, H.A., Romanelli, G.P., Martinez, J.J., and Luque, R. (2020) Production of 5-hydroxymethyl-2-furan carboxylic acid by *Serratia marcescens* from crude 5-hydroxymethylfurfural. *Biochem Eng J* **154:** 107421.

Petkovic, M., Ferguson, J., Bohn, A., Trindade, J., Martins, I., Carvalho, M.B., *et al.* (2009) Exploring fungal activity in the presence of ionic liquids. *Green Chem* **11:** 889–894.

van Putten, R.J., van der Waal, J.C., de Jong, E., Rasrendra, C.B., Heeres, H.J., and de Vries, J.G. (2013) Hydroxymethylfurfural, a versatile platform chemical made from renewable resources. *Chem Rev* **113:** 1499–1597.

Rajesh, R.O., Godan, T.K., Rai, A.K., Sahoo, D., Pandey, A., and Binod, P. (2019) Biosynthesis of 2, 5-furan dicarboxylic acid by *Aspergillus flavus* APLS-1: process optimization and intermediate product analysis. *Bioresour Technol* **284:** 155–160.

Ran, H., Zhang, J., Gao, Q., Lin, Z., and Bao, J. (2014) Analysis of biodegradation performance of furfural and 5-hydroxymethylfurfural by *Amorphotheca resinae* ZN1. *Biotechnol Biofuels* **7:** 51.

Resasco, D.E., Sitthisa, S., Faria, J., Prasomsri, T., and Ruiz, M.P. (2015) Furfurals as chemical platform for biofuels production. In *Solid Waste as a Renewable Resource Methodologies*. Albanese, J.A.F., and Ruiz, M.P. (eds). Oakville, ON, Canada: Apple Academic Press, Inc, p. 103.

Rosatella, A.A., Simeonov, S.P., Frade, R.F.M., and Afonso, C.A.M. (2011) 5-Hydroxymethylfurfural (HMF) as a building block platform: biological properties, synthesis and synthetic applications. *Green Chem* **13:** 754.

Seifert, K., Hughes, S., Boulay, H., and Louis-Seize, G. (2007) Taxonomy, nomenclature and phylogeny of three cladosporium-like hyphomycetes, Sorocybe resinae, Seifertia azaleae and the Hormoconis anamorph of *Amorphotheca resinae*. *Stud Mycol* **58:** 235–245.

Stajich, J.E., Harris, T., Brunk, B.P., Brestelli, J., Fischer, S., Harb, O.S., *et al.* (2012) FungiDB: an integrated functional genomics database for fungi. *Nucleic Acids Res* **40:** D675–D681.

Surh, Y.-J., and Tannenbaum, S.R. (1994) Activation of the Maillard reaction product 5-(hydroxymethyl) furfural to strong mutagens via allylic sulfonation and chlorination. *Chem Res Toxicol* **7:** 313–318.

Taherzadeh, M.J., Gustafsson, L., Niklasson, C., and Lidén, G. (2000) Inhibition effects of furfural on aerobic batch cultivation of *Saccharomyces cerevisiae* growing on ethanol and/or acetic acid. *J Biosci Bioeng* **90:** 374–380.

Voutchkova-Kostal, A.M., Kostal, J., Connors, K.A., Brooks, B.W., Anastas, P.T., and Zimmerman, J.B. (2012) Towards rational molecular design for reduced chronic aquatic toxicity. *Green Chem* **14:** 1001–1008.

Wang, L., Wu, D., Tang, P., and Yuan, Q. (2013) Effect of organic acids found in cottonseed hull hydrolysate on the xylitol fermentation by *Candida tropicalis*. *Bioprocess Biosyst Eng* **36:** 1053–1061.

Wang, W., Yang, S., Hunsinger, G.B., Pienkos, P.T., and Johnson, D.K. (2014) Connecting lignin-degradation pathway with pre-treatment inhibitor sensitivity of *Cupriavidus necator*. *Front Microbiol* **5:** 247.

Wang, X., Gao, Q., and Bao, J. (2015) Transcriptional analysis of *Amorphotheca resinae* ZN1 on biological degradation of furfural and 5-hydroxymethylfurfural derived from lignocellulose pretreatment. *Biotechnol Biofuels* **8:** 136.

Xiao, Z., Zhang, X., Gregg, D.J., and Saddler, J.N. (2004) Effects of sugar inhibition on cellulases and β-glucosidase during enzymatic hydrolysis of softwood substrates. In *Proceedings of the Twenty-Fifth Symposium on Biotechnology for Fuels and Chemicals Held May 4–7, 2003*. Breckenridge, CO: Springer, pp. 1115–1126.

Yates, A.D., Achuthan, P., Akanni, W., Allen, J., Allen, J., Alvarez-Jarreta, J., *et al.* (2020) Ensembl 2020. *Nucleic Acids Res* **48:** D682–D688.

Yi, X., Gao, Q., Zhang, L., Wang, X., He, Y., Hu, F., *et al.* (2019) Heterozygous diploid structure of *Amorphotheca resinae* ZN1 contributes efficient biodetoxification on solid pretreated corn stover. *Biotechnol Biofuels* **12:** 126.

Yuan, H., Liu, H., Du, J., Liu, K., Wang, T., and Liu, L. (2020) Biocatalytic production of 2, 5-furandicarboxylic acid: recent advances and future perspectives. *Appl Microbiol Biotechnol* **104:** 527–543.

Zhang, D., and Dumont, M.J. (2017) Advances in polymer precursors and bio-based polymers synthesized from 5-hydroxymethylfurfural. *J Polym Sci A Polym Chem* **55:** 1478–1492.

Supporting information

Additional supporting information may be found online in the Supporting Information section at the end of the article.

Data S1. Full LC-ESI-MS data of the OBMF extracellular medium containing.

Data S2. Full orthology data obtained for 25 fungal genomes using OrthoFinder.

Data S3. Gene tree of the AN4212 orthogroup generated upon OrthoFinder analysis.

Data S4. Gene tree of the AN7164 orthogroup generated upon OrthoFinder analysis.

Data S5. Protein sequence alignments comparing selected proteins of the AN4212 orthogroup with their homologous in *C. basilensis* – hmfH.

Data S6. Protein sequence alignments comparing selected proteins of the AN7164 orthogroup with their homologous in *C. basilensis* – hmfF.

Fig. S1. Fresh weight of mycelia after incubation in control conditions (white bar), with HMF, BHMF, FDCA and OBMF. Statistically significant differences relative to the control are marked with an asterisk.

Fig. S2. Biotransformation of HMF. HPLC chromatogram of the abiotic control of HMF (A) and after 14 days of incubation at the intra (B) and extracellular (C) fractions. The NMR spectra at the 1st (D and E) and 14th (F and G) days of incubation are also depicted for the extra (D and F) and intracellular (E and G) fractions.

Fig. S3. Biotransformation of BHMF. HPLC chromatogram of the abiotic control of BHMF (A) and after 14 days of incubation at the intra (B) and extracellular (C) fractions. The NMR spectra at the 1st (D and E) and 14th (F and G) days of incubation are also depicted for the extra (D and F) and intracellular (E and G) fractions.

Fig. S4. Biotransformation of FDCA. HPLC chromatogram of the abiotic control of FDCA (A) and after 14 days of incubation at the intra (B) and extracellular (C) fractions. The NMR spectra at the 1st (D and E) and 14th (F and G) days of incubation are also depicted for the extra (D and F) and intracellular (E and G) fractions.

Fig. S5. Biotransformation of OBMF. HPLC chromatogram of the abiotic control of OBMF (A) and after 14 days of incubation at the intra (B) and extracellular (C) fractions. The NMR spectra at the 1st (D and E) and 14th (F and G) days of incubation are also depicted for the extra (D and F) and intracellular (E and G) fractions.

Fig. S6. *In-vitro* decay of FDCA in the presence or absence of glucose. The ability of pyruvate decarboxylase (A and B) and cellulase (C and D) to promote the decay of FDCA in the presence (A and C) or absence (B and D) of glucose is shown.

Fig. S7. TIC profile of the OBMF sample after 14 days of incubation with *A. nidulans*, obtained using LC/MS.

Fig. S8. MS spectrum of the peak at 3.514 minutes. For the targeted analysis, compound 1 was synthesized (see below), and its MS/MS spectrum was used to confirm the identification. Therefore, positive results were obtained for compound 1 (5-{[(5-formylfuran-2-yl)methoxy]methyl}furan-2-carboxylic acid), with a confidence level of 96.6% relative to the standard compound (see below).

Fig. S9. MS spectrum of the synthesized standard of compound 1 (see details below).

Fig. S10. MS spectrum of the peak at 3.362 minutes. For the targeted analysis, compound 1 was synthesized (see below), and its MS/MS spectrum was used to confirm the identification. Therefore, positive results were obtained for compound 2 (5-({[5-(hydroxymethyl)furan-2-yl]methoxy} methyl)furan-2-carboxylic acid), with a confidence level of 98.7% relative to the standard compound (see below).

Fig. S11. MS spectrum of the synthesized standard of compound 1 (see details below).

Fig. S12. ^{1}H NMR spectra of compound 1

Fig. S13. ^{13}C NMR spectra of compound 1

Fig. S14. ^{1}H NMR spectra of compound 2

Fig. S15. ^{13}C NMR spectra of compound 2

Fig. S16. Protein domains of the *hmfF* gene of *C. basilensis*, obtained upon InterProScan analysis.

Fig. S17. Protein domains of the AN7164 gene of *A. nidulans*, obtained upon InterProScan analysis.

Fig. S18. Protein domains of the *hmfG* gene of *C. basilensis*, obtained upon InterProScan analysis.

Fig. S19. Protein domains of the AN12147 gene of *A. nidulans*, obtained upon InterProScan analysis.

Fig. S20. Protein domains of the *hmfH* gene of *C. basilensis*, obtained upon InterProScan analysis.

Fig. S21. Protein domains of the AN4212 gene of *A. nidulans*, obtained upon InterProScan analysis.

Fig. S22. Confirmation of gene replacement for AN4212 mutant strain. The expected amplification products of diagnostic PCR and their digestion with restriction enzymes BglII and NdeI are represented for the wild-type strain (A) and the obtained mutant (B). Gel electrophoresis (1% agarose) of the diagnostic PCR and digestion products confirm the correct gene replacement in the mutant strain (C). Due to low resolution in the agarose gel, digestion products smaller than 500 bp were not considered as main products.

Fig. S23. Confirmation of gene replacement for AN7164 mutant strain. The expected amplification products of diagnostic PCR and their digestion with restriction enzymes BglII and NdeI are represented for the wild-type strain (A) and the obtained mutant (B). Gel electrophoresis (1% agarose) of the diagnostic PCR and digestion products confirm the correct gene replacement in the mutant strain (C). Due to low resolution in the agarose gel, digestion products smaller than 500 bp were not considered as main products.